

BEST  
AVAILABLE COPY

Approved for public release;  
Distribution unlimited

ENVPREDRSCHFAC ✓  
Technical Paper No. 13-74

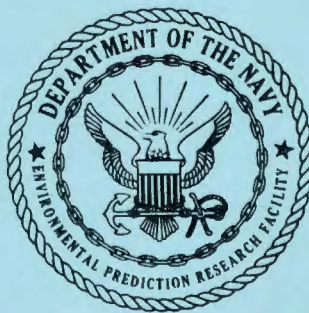
U. S. Dept. of the Navy

**THE EFFECT OF UTILIZING  
EMPIRICALLY DERIVED VALUES OF  
COALESCENCE EFFICIENCY IN  
A MICROPHYSICAL CLOUD MODEL**

by

**PAUL M. TAG**

**SEPTEMBER 1974**



*U.S. Navy*

**ENVIRONMENTAL PREDICTION RESEARCH FACILITY**

**NAVAL POSTGRADUATE SCHOOL  
MONTEREY, CALIFORNIA 93940**

BEST  
AVAILABLE COPY

Qualified requestors may obtain additional copies from the Defense Documentation Center. All others should apply to the National Technical Information Service.

ENVIRONMENTAL PREDICTION RESEARCH FACILITY  
NAVAL POSTGRADUATE SCHOOL  
MONTEREY, CALIFORNIA 93940

20x4

IN REPLY REFER TO

EPRF/KGR:wc  
5605

Ser: 815

20 SEP 1974

RECEIVED

OCT 03 1974

From: Commanding Officer  
To: Distribution List

**Office of the Director**

Subj: Meteorological Research Publication; forwarding of

Encl: (1) "The Effect of Utilizing Empirically Derived Values of Coalescence Efficiency in a Microphysical Cloud Model," ENVPREDRSCHFAC Tech. Paper No. 13-74, September 1974

1. Enclosure (1) is forwarded for information.

*J. D. Mackenzie*

J. D. MACKENZIE  
By direction

Distribution List:

Environmental Prediction Research Facility Master Distribution List of 15 May 1974.

LIST II: SNDL Nos. A2A (items 1, 2, 4, 5, 8, 9, and 10), A3 (item 2), A4A (item 2), B2 (items 1 and 2), C4F7 (item 4), C4J (items 1, 2, and 3), C4L, E3A (items 1, 2, 3, and 5), E3B (items 1, 2, and 3), FF38 (items 1 and 2), FF42 (items 1, 2, 3 and including Prof. W. Reese and Prof. G. Schacher, NAVPGSCOL), FKALA (items 1, 2, 4, and 5), FKA6A2 (including Dr. R.F. Reinking, NWC, China Lake), FKA6A8, FT5, FT13, and FW1.

LIST III: Item Nos. 1, 2, 3, 4, 6, 8, and 14.

LIST IV: Item Nos. 1, 2, 4, 5, 6, 7, and 9.

LIST V: Item Nos. 1, 2, and 4.

LIST VII: Item Nos. 1, 2, 5, 6, 8, 9, 10, 11, 14, 15, 17, 18, 19, 20, 21, 22, 25, 26, 30, 37, and including Dr. R.L. Lavoie, NOAA,

LIST VIII: Item Nos. 1, 2, 3, 4, 5, 6, 7, 9, 14, and including Dr. E. Berry, National Science Foundation.

LIST IX: Item Nos. 1, 3, 5, 6, 7, 8, 9, 10, 14, 16, 17, 20, 21, 22, 23, 24, 27, 28, 31, 32, 33, 34, 35, 36, 37, 38, 39, 40, 41, 42, 50, 64, and including: Mr. D. Johnson, University of Chicago, Dr. S. C. Lee, University of Missouri and Mr. E. Hindman, University of Washington.

LIST X: Item Nos. 1, 3, 4, 5, 6, 10, 11, 12, 14, 15, 27, 31, and including: Mr. H. Wilkinson, McDonnell Douglas Astro. Co.

LIST XI: Item Nos. 1 and 2.

LIST XII: Item Nos. 1, 5, 6, and 8.

LIST XIII: Item Nos. AUS-1, CAN-1, GER-1, and 2, ISR-1, JAP-1, NOR-1 and 3, SWE-1 and 3.



20. (continued)

coalescence efficiency to be equal to one, the recent work of Whelpdale and List, and Levin et al., indicate that coalescence efficiency is closely related to droplet/drop size ratio  $P$ , and decreases with increasing  $P$ . Starting with an initial droplet spectrum for a tropical cumulus which produces rain within 20 minutes when using a coalescence efficiency of one, comparative runs are made using the empirical data. Utilization of these efficiencies leads to delay of precipitation and to decreases both in rainfall intensity and cumulative rainfall. Using the more restrictive of the two sets of efficiency data considered forces liquid water contents to be unreasonably large in order to sufficiently stimulate the coalescence mechanism.

CONTENTS

ACKNOWLEDGMENTS . . . . . 2

1. BACKGROUND AND INTRODUCTION . . . . . 3

2. MODEL DESCRIPTION AND NUMERICAL PROCEDURE . . . . . 9

    1. BASIC MODEL DESCRIPTION . . . . . 9

    2. THE DIFFERENTIAL EQUATION . . . . . 9

    3. DROPLET CATEGORIES . . . . . 11

    4. SOLUTION OF THE DIFFERENTIAL EQUATION . . . . . 12

    5. DROPLET TERMINAL VELOCITIES . . . . . 13

    6. COLLISION-COALESCENCE OF DROPLETS . . . . . 13

    7. ACCURACY OF COALESCENCE SCHEME . . . . . 17

    8. COLLISION AND COALESCENCE EFFICIENCIES . . . . . 19

    9. DROP BREAKUP . . . . . 21

    10. COMPUTATIONAL PROCEDURE . . . . . 22

3. INITIAL CLOUD CONDITIONS . . . . . 24

4. MODEL RESULTS . . . . . 26

5. SUMMARY AND CONCLUSIONS . . . . . 34

6. REFERENCES . . . . . 35

## ACKNOWLEDGMENTS

The author is indebted to the many members of the Environmental Prediction Research Facility who assisted in this work, particularly Miss Margaret Humbracht who provided several valuable suggestions regarding the paper's content.

## 1. BACKGROUND AND INTRODUCTION

Langmuir (1948), Bowen (1950), and Ludlam (1951) early suggested that collision-coalescence could be a dominating mechanism in producing rain from a warmer than freezing cloud. It was recognized that a few cloud droplets, after having grown to a size larger than the average cloud droplet, would fall faster, and also sweep out cloud droplets more efficiently. Findeisen (1939) had earlier considered this mechanism, but doubted its efficiency. He and Bergeron (1935) instead emphasized mixed-phase growth (ice and water) when clouds extended above the 0°C isotherm.

By calculating values for the collision efficiency, Langmuir showed how a chain reaction could initiate precipitation after seeding with large water drops. Both Bowen and Ludlam then suggested and demonstrated that precipitation could result naturally in isolated warm convective clouds. Bowen, however, concluded that, based on his trajectory calculations, rain could not form in times less than 60 minutes. He realized that this conclusion was contrary to observation in that most convective clouds go through a growth-dissipation cycle in times much less than 60 minutes. Ludlam concluded that collision-coalescence is probably effective only in maritime clouds, where there is more opportunity for initial formation of droplets greater than 20  $\mu\text{m}$  radius.

Because rain obviously could be produced in warm clouds in times less than an hour, other methods of enhancing the coalescence process were suggested. Cochet (1951) showed how droplet charging could provide stimulation to the collection process, while East and Marshall (1954) suggested that turbulence could increase collection efficiencies.

Recognizing the importance of collision efficiency values for these theoretical studies, Pearcey and Hill (1956) extended the work of Langmuir by calculating collision efficiencies

for droplets of comparable size up to 200  $\mu\text{m}$  radius. They neglected, however, interaction of each droplet's flow field on that of the other. Hocking (1959) concluded that such an approximation was in error for droplets remaining near each other for a period of time (droplets similar in size). He removed the approximation and recalculated efficiencies for radii up to 30  $\mu\text{m}$ . His results differed from Pearcey and Hill in that he found a limiting upper size that a droplet can collect, whereas the former found collision efficiency to increase as the ratio of the two radii increased to one. The most significant conclusion of Hocking, however, was that a droplet of radius less than 18  $\mu\text{m}$  could not be a collecting drop, i.e., that its collision efficiency is zero. This conclusion was to be accepted for several years.

At about the same time that theoretical studies were initiated, laboratory investigations to determine empirical values for collection efficiencies were being conducted. Gunn and Hitschfeld (1951) computed growth rates for 1.59 mm radius drops falling through three cloud droplet size spectra. They found that the collection efficiencies calculated from these growth rates were in agreement with the theoretical work of Langmuir. They concluded, at least in the size ranges they considered, that coalescence efficiency is equal to one. Sartor (1954) conducted experiments involving small droplets of similar size (distilled water falling in mineral oil). He found that collision efficiencies for sizes from 5 to 15  $\mu\text{m}$  radius were larger than those calculated by Langmuir. Telford et al. (1955) also attempted to determine the efficiencies of droplets nearly equal in size. They found that such droplets, at least in the size range 75  $\mu\text{m}$  and larger, do have a high probability of colliding and attributed this result to wake effect to the rear of the leading drop.

Schotland and Kaplin (1956) conducted experiments using small steel spheres falling in a sugar solution. They found

finite values of collision efficiency for sizes of 5.5, 7.0, 8.5, and 10.5  $\mu\text{m}$  radius. This result was to be in contradiction to Hocking's theoretical conclusions two years later. Hocking concluded, however, that these empirical results were not representative of conditions in air. Telford and Thorndike (1961) gave added impetus to Hocking's claim when their results indicated that collisions involving droplets of about 35  $\mu\text{m}$  diameter were very rare.

Further refinements to theoretically calculated collision efficiencies came in the sixties. Shafrir and Neiburger (1963) extended the work of Hocking by calculating efficiencies for radii up to 136  $\mu\text{m}$ . Davis and Sartor (1967) provided the most significant contribution when, after making further refinements to Hocking's method of calculation, they found that there was no cutoff below 18  $\mu\text{m}$  as Hocking had found. Collision efficiencies, although small, were finite. This was a significant finding.

Although theory had become increasingly refined, laboratory work gave conflicting results. Collision efficiencies were not always verified. As several of the early researchers had suggested, however, the difficulty might lie in the fact that all collisions do not necessarily result in coalescences, i.e., coalescence efficiency is not equal to one. Magono and Nakamura (1959) photographed collisions between a large stationary water drop and smaller colliding droplets. They found that coalescence and rupturing of the larger drop is a function of the smaller droplet's size. By projecting 100-400  $\mu\text{m}$  radius drops on a large liquid hemispherical surface, Schotland (1960) ascertained that coalescence was related to two dimensionless parameters. These parameters are a function of drop density, medium density, surface tension, normal component of impact velocity, and drop diameter. By impacting water droplets with radii of 60 to 200  $\mu\text{m}$  on a plane water surface, Jayaratne and Mason (1964) found that coalescence is a function of the angle of impact and

that larger drops coalesce at smaller impact angles.

More recently, Whelpdale and List (1971) observed collisions between a raindrop-size drop (500-1750  $\mu\text{m}$  radius) and a droplet of cloud droplet size (35  $\mu\text{m}$  radius). They determined that coalescence occurs for 85-95% of collisions for those cases where impact velocity was equivalent to the difference in their terminal velocities. As others had also found, a barrier to coalescence is the film of air which exists between the colliding drops. Based on their observations, they found that the expression  $E = r_i^2 / (r_i + r_n)^2$ , where E is the coalescence efficiency,  $r_i$  the radius of the large drop, and  $r_n$  the small droplet radius, is valid for drop radii  $400 < r_i < 2000 \mu\text{m}$  and droplet radii  $20 < r_n < 100 \mu\text{m}$ .

The experiments of Whelpdale and List concentrated only on rather small droplet/drop (collected/collector) ratios, and then only for rather large collector drops. Based on their data, there was no evidence to suggest that their formula was really valid for increasing size ratios. Levin et al. (1973) helped fill this gap. Using collector drops averaging in radius from 50 to 100  $\mu\text{m}$  and the collision efficiency data of Shafrir and Neiburger (1963), they computed coalescence efficiencies for droplet/drop ratios of 0.18, 0.20, 0.22, and 0.24. Although their values fall below the curve suggested by Whelpdale and List, the trend is the same -- decreasing values of coalescence efficiency with increasing size ratios. Feeling that this trend is quite real, Levin et al., suggested that, for large size ratios, previous results in which collection efficiencies agreed with computed collision efficiencies probably reflect enhanced coalescence through droplet charging caused by the experimental techniques used.

Since the continuous growth calculations of Bowen (1950) and Ludlam (1951), inclusion of the stochasticity of the collection process in numerical computations has provided an explanation as to how collision-coalescence can lead to rain

within 20 to 30 minutes. Telford (1955) was the first to make the suggestion that a discrete, chain reaction type process could lead to rapid growth of a small fraction of drops. All earlier growth computations had assumed continuous growth whereby all droplets of a given initial size grew equally with time. Extending Telford's work which considered only two initial categories of drops, Twomey (1964) studied the evolution of a spectrum of cloud droplets. In general agreement with Telford, he found that production of a few large drops proceeds about ten times faster than computations involving continuous growth. Bartlett (1966) concentrated on the growth region from 20 to 40  $\mu\text{m}$  radius and determined the effect of small changes in the collection efficiencies -- changes which were to simulate electrical or turbulent effects. He found that any external alteration which produces changes of less than 10% can be ignored. In an important paper, Berry (1967) added considerable depth to the study of droplet collection. One of his conclusions was that continuous growth is important initially, before a second spectrum maximum of water mass is formed. Thereafter, stochastic growth becomes increasingly important.

New computers of increased speed and size have enabled researchers to utilize collection equations in cloud models. Many of these models emphasized the dynamics of clouds (e.g., Simpson and Wiggert, 1969; and Weinstein, 1970) and utilized parameterized microphysics as developed either by Kessler (1969) or Berry (1968). Others, however, did include explicit coalescence growth: Nelson (1971), for the purpose of developing rain from an isolated tropical cumulus with a time-independent updraft profile; Takeda (1971), in a two-dimensional model which concentrated on the effect of an environmental vertical wind profile; and Danielsen et al. (1972), for the purpose of generating hail. Silverman and Glass (1973) showed that the results of parameterized microphysics in cloud models are

significantly different from those involving detailed explicit microphysical calculations.

Implicit in all of the above cited studies is the assumption that the collection efficiencies are identically equal to the utilized collision efficiencies. The purpose of this paper is to report the results of an investigation into the effect of utilizing the empirical data of Whelpdale and List, and Levin et al. for the coalescence efficiencies. The investigation was done by means of a time-dependent eulerian model of stochastic coalescence, drop breakup, and vertical mass transfer. By utilizing the coalescence efficiencies in the model it is possible to determine to what extent reduction of collection efficiency delays the onset of precipitation initiated by stochastic coalescence, an onset that can be demonstrated to occur within the necessary time frame by existing theory, but a theory that assumes that all collisions result in coalescences. If the delay is significant, efforts should be directed toward other positive effects such as electrically enhanced coalescence. At the least, it should suggest continued empirical studies of coalescence efficiency.

## 2. MODEL DESCRIPTION AND NUMERICAL PROCEDURE

### 1. BASIC MODEL DESCRIPTION

The basic design of the model is very similar to that of Nelson (1971). It is one-dimensional with ten levels in the vertical. The purpose of the model is not to simulate initial cloud development nor to model the dynamic aspects of cloud growth. It was designed for studying the micro-physical aspects of droplet growth in a tropical warm cumulus. For this purpose a droplet spectrum is prescribed initially at each of the model's ten levels and allowed to evolve by stochastic coalescence, drop breakup, and droplet fallout. As suggested by Nelson, a time-independent updraft profile is utilized to provide a way of accumulating water in the upper regions of the cloud and to provide a realistic restraint for hydrometeor fallout.

Forty-nine categories of droplet size are utilized for spectrum description -- ranging from one to 2820  $\mu\text{m}$  radius in a logarithmic progression. As the spectrum evolves in time, droplets enter category sizes with terminal velocities exceeding the updraft, and exit the cloud base as rain. A special array is utilized to store this fallout in order to examine its characteristics.

### 2. THE DIFFERENTIAL EQUATION

Let  $N(r,z,t)$  be the average number of droplets of radius  $r$ , at a height  $z$ , and time  $t$  (definitions of symbols are given in Table 1). The partial differential equation which then describes the processes given above is

$$\frac{\partial N(r,z,t)}{\partial t} = \frac{-\partial}{\partial z} [N(r,z,t) (w(z) - u(r,z))] + Q(r,z,t) + \beta(r,z,t), \quad (1)$$

Table 1. Definition of Symbols

b	Constant used in Golovin collection kernel ( $1500 \text{ sec}^{-1}$ )
B	Partitioning factor for "splitting" scheme (dimensionless)
B1	Partitioning factor for linear "splitting" of droplet number (dimensionless)
B2	Partitioning factor for logarithmic "splitting" of droplet mass (dimensionless)
E(i,n)	Coalescence Efficiency (dimensionless)
f(lnr)	Number of droplets as a function of lnr ( $\text{no. m}^{-3}$ )
i,n	Droplet category indicators
M	Total number of droplet categories
$N_0$	Initial droplet concentration ( $\text{no. m}^{-3}$ )
$N(r,z,t)$	Droplet concentration ( $\text{no. m}^{-3}$ ) as a function of r,z,t
P(i,n)	Collection probability of an ith category droplet collecting an nth category droplet
Q	Source/sink term symbolizing collision-coalescence
$r_i$	Radius of droplet of category i (cm)
t	Time (sec)
V(i,n)	Collection kernel as a function of the ith and nth category droplets ( $\text{cm}^3 \text{ sec}^{-1}$ )
$v_0$	Mean volume of the droplet spectrum at $t = 0$ ( $\text{cm}^3$ )
$v(r)$	Volume of a droplet of radius r ( $\text{cm}^3$ )
x	Maximum distance from the collector drop's center (measured perpendicular to the line of fall) outside of which no collision would occur (cm)
$X_1, X_2$	Mass conversion factors used in coalescence equation (dimensionless)
$Y_c$	Linear collision efficiency (dimensionless)
z	Height (m)
$\beta$	Source/sink term symbolizing drop breakup
$\gamma$	Multiplicative factor for logarithmic droplet sequence
$\mu\text{m}$	Micron ( $10^{-4}$ cm)

where  $w(z)$  is the updraft speed,  $u(r,z)$  is the terminal velocity of a droplet of radius  $r$  at height  $z$ ,  $Q$  is a source/sink term to account for collision-coalescence, and  $\beta$  is a source/sink term for drop breakup.

### 3. DROPLET CATEGORIES

The process of stochastic coalescence, operating on only a small initial number of different sized drops, by definition, results in a myriad of new size combinations after just several time steps. It is physically difficult to keep track of all combinations for very long. As a result, Eq. (1) is solved at each of the ten levels for a sequence of fixed radii. For the process of collision-coalescence and drop breakup, newly created droplets of different size are refit back into the fixed discrete sizes. The fitting procedure will be described in the following section.

Because of the range of droplet sizes (usually one  $\mu\text{m}$  to several thousand  $\mu\text{m}$  radius) that are typically covered in a microphysical model, care must be taken in choosing a size sequence. A linear sequence of discrete sizes is not practical. For example, even a five  $\mu\text{m}$  separation results in 200 categories for a 1000  $\mu\text{m}$  maximum size. Ten levels thus results in 2000 solutions to Eq. (1) in one time step. The complexity of the coalescence calculations makes such a sequence impractical.

A more workable sequence is a logarithmic one which allows good resolution at the smallest sizes where it is generally needed, but also permits inclusion of the larger precipitation-size drops if they should be needed. The discrete sequence that was chosen progresses according to Eq. (2).

$$r_j = \gamma r_{j-1} \quad (2)$$

The subscript  $j$  designates droplet category, and  $r_1$ , the smallest radius, is 1  $\mu\text{m}$ .

Eq. (3) describes a desirable criterion for  $\gamma$ .

$$r_j^3 + (\gamma r_j)^3 \leq (\gamma^2 r_j)^3 \quad (3)$$

Such a restriction allows no droplet size combinations (resulting from coalescence) to advance past one category greater than the largest of the two combining droplets. The cube is significant because liquid water is proportional to radius cubed.

The factor  $\gamma$  can be determined by solving Eq. (3).

Letting  $r_j = r_1 = 1 \mu\text{m}$ , we have

$$(1)^3 + \gamma^3 \leq \gamma^6. \quad (4)$$

By using an equality for a solution and letting  $\gamma^3 = A$ , we have

$$A^2 - A - 1 = 0. \quad (5)$$

Utilizing the quadratic formula produces one real positive solution,  $A = 1.618$ . The cube root of  $A$  yields  $\gamma = 1.174$ . This value of  $\gamma$  produces the equality; hence a correct two-place inequality results from 1.18.

Consequently, we arrive at a numerical sequence of radii: 1.00, 1.18, 1.39, 1.64, etc. Presently, 49 droplet categories are utilized in the model. This number permits a maximum radius of 2820  $\mu\text{m}$ , the size at which drop breakup is permitted to occur.

#### 4. SOLUTION OF THE DIFFERENTIAL EQUATION

By recognizing that the processes described in Eq. (1) are independent of one another allows each process to be solved separately in each time step (for each droplet category), and then summed to produce the total change in  $N(r,z,t)$ , the primary output of the model. Such separation is desirable because of the complexity of the coalescence computations. An explicit finite-difference scheme is used for the advective term.

Because  $Q$  and  $\beta$  can be considered as constants in Eq. (1), the stability criteria for advection then determines total stability.

Time derivatives are forward differenced while the "donor cell" or flux method of advection is used for the spatial derivative (Thoman and Szewczyk, 1966). This form of the space derivative allows for mass conservation and takes the form

$$\frac{\partial [N(w - u)]}{\partial z} = \frac{N^Z(w^Z - u^Z) - N^{Z-1}(w^{Z-1} - u^{Z-1})}{\Delta z} . \quad (6)$$

## 5. DROPLET TERMINAL VELOCITIES

The mathematical approximations of Wobus et al. (1971) are used for the droplet terminal velocities. These approximations allow for terminal velocity calculation as a continuous function of droplet radius; they are in excellent agreement with Stoke's law for radii smaller than 50  $\mu\text{m}$ , and with the data of Gunn and Kinzer (1949) for larger drops at standard air density and viscosity. Because the terminal velocities in this model are to apply at heights considerably above the ground, the effect of non-standard atmospheric conditions is included. Consequently, the velocity of a droplet changes slightly from cloud base to cloud top. These velocities are calculated once at the start of the program and stored in a two-dimensional array for later use. The collection kernel (to be described later) is also dependent upon these velocities.

## 6. COLLISION-COALESCENCE OF DROPLETS

The important relevant process simulated in this study is collision-coalescence -- the term  $Q$  in Eq. (1). For a given level and time, the change in droplet number due to stochastic

coalescence is

$$\begin{aligned}
 Q(r_i)\Delta t = & -N(r_i) \sum_{n=1}^{i-1} P(i,n) - \sum_{n=i+1}^M N(r_n) P(n,i) \\
 & + N(r_i) \sum_{n=1}^{i-1} P(i,n) X_1(i,n) (1 - B(i,n)) \\
 & + N(r_{i-1}) \sum_{n=1}^{i-2} P(i-1,n) X_2(i,n) B(i-1,n), \quad (7)
 \end{aligned}$$

where  $i$  and  $n$  both refer to category numbers,  $M$  is the total number of categories,  $P(i,n)$  is the collection probability,  $B(i,n)$  is the partitioning factor, and  $X_1$ ,  $X_2$  are mass conversion factors, necessary if mass is partitioned.

$P(i,n)$  is the collection probability, the probability that an  $i^{\text{th}}$  droplet will collide and coalesce with an  $n^{\text{th}}$  droplet in time  $\Delta t$ :

$$P(i,n) = V(i,n) E(i,n) N(r_n)\Delta t \quad (8)$$

where  $V(i,n)$ , as defined by Berry (1967), is the collection kernel:

$$V(i,n) = \pi r_i^2 Y_c (r_i, r_n)^2 (w(r_i) - w(r_n)). \quad (9)$$

$Y_c$  is the linear collision efficiency used by Shafrir and Neiburger (1963). As defined earlier,  $u(r,z)$  is the terminal velocity of a droplet, and  $E(i,n)$  is the coalescence efficiency which will be considered separately.

The collection kernel describes the effective rate at which volume is swept out by the collector drop. It is a function of the area through which the collector drop falls ( $\pi r_i^2$ ), the difference between its own terminal velocity and that of the droplet it is collecting ( $u(r_i,z) - u(r_n,z)$ ), and the efficiency with which droplets are swept from that volume ( $Y_c^2$ ). This collision efficiency is defined as:

$$Y_c^2 = \frac{\pi X^2}{\pi r_i^2} \quad (10)$$

where  $x$  is that maximum distance from the collector drop's center (measured perpendicular to the direction of fall) outside of which a collision would not occur (Fletcher, 1962).

The partitioning factor  $B$  determines how droplet mass or number is split between droplet categories as it is "advected" into larger radii categories as the result of collision-coalescence. The adoption of a partitioning scheme was originally stimulated by Bartlett (1966) and is similar to that of Kovetz and Olund (1969) who used

$$B(i,n) = B1(i,n) = \frac{(r_i^3 + r_n^3) - r_i^3}{r_{i+1}^3 - r_i^3} = \frac{r_n^3}{r_{i+1}^3 - r_i^3} \quad (11)$$

for partitioning of droplet number. Since, in this case, droplet number is being redistributed, the conversion factors  $X_1$  and  $X_2$  are unnecessary and are set equal to one. The advantage of this scheme is that both number and mass are conserved. Unfortunately, it leads to an unrealistic pseudo-diffusion of mass such that the solution is "fast." Depending on the purpose, such diffusion may not be significant. However, in the current situation where the time-development of precipitation is the critical outcome, the diffusion was considered unacceptable. Consequently, a more accurate solution was sought.

After a trial and error examination of several splitting schemes, the desired accuracy (to be demonstrated in the following section) was found with a logarithmic partitioning of droplet mass, instead of a linear partitioning of droplet number:

$$B(i,n) = B2(i,n) = \frac{\xi(i,n) - r_i^3}{r_{i+1}^3 - r_i^3}, \quad (12)$$

where  $\xi(i,n) = \exp[\ln r_i^3 + B1(i,n) (\ln r_{i+1}^3 - \ln r_i^3)]$  (13)  
 and  $B1(i,n)$  is that defined in Eq. (11). By recognizing  
 that  $r_{i+1} = \gamma r_i = 1.18 r_i$ , Eq. (13) reduces to

$$\xi(i,n) = r_i^3 (\gamma^3)^{B1(i,n)} = r_i^3 (1.643032)^{B1(i,n)}. \quad (14)$$

It should be recognized that Eq. (12) represents nothing more  
 than the logarithmic position (between the two discrete droplet  
 sizes) of the newly created droplet mass, rather than the  
 linear position given in Eq. (11).

Because mass would not be conserved if droplet number  
 were partitioned according to Eq. (12), mass must be partitioned  
 instead. Consequently, the mass conversion factors  $X_1$  and  
 $X_2$  are necessary for droplet number recomputation:

$$X_1(i,n) = \frac{r_i^3 + r_n^3}{r_i^3}; \quad X_2(i,n) = \frac{r_{i-1}^3 + r_n^3}{r_i^3}. \quad (15)$$

Droplet number is now not conserved, but as will be shown in  
 the following section, spectrum mass evolution is much better.

Equation (7) is solved for category numbers  $i = 3$  to  
 $i = M-1$ . Categories 1, 2, and  $M$  are special cases and must be  
 considered separately since they fall on the ends of the distri-  
 bution, resulting in the loss of several of the terms in Eq. (7).  
 Eq. (7) allows for all combinations of collisions that either  
 increase or diminish the number of droplets in a category. The  
 only overriding restriction is that one droplet can have but  
 one collision per time step. The first term in Eq. (7) allows  
 a droplet to be removed because of a collision with a droplet  
 smaller than itself. The second term allows for loss due to  
 larger collecting drops. The third term allows for a  
 droplet to re-enter that size category from partitioning  
 resulting from collisions that itself incurs (thus producing  
 a droplet size that must be partitioned between itself and the  
 next largest category). The fourth term allows for re-entry

resulting from collisions incurred by the next smallest category (producing a droplet of a size between itself and the category in question). By utilizing the criteria imposed by Eq. (3) there is no danger of droplets entering a category from sources other than those described above.

## 7. ACCURACY OF COALESCENCE SCHEME

In order to test the accuracy of any scheme it is necessary to compare the results of a given case with a known exact solution of that same case. Golovin (1963) was the first to derive an exact analytic solution for one limited case -- one in which the collection kernel was proportional to the droplet volumes:

$$V(i,n) = b\left(\frac{4}{3}\pi\right) (r_i^3 + r_n^3) \quad (16)$$

where  $b$  is a constant ( $1500 \text{ sec}^{-1}$ ). Scott (1968) later provided analytic solutions for other specific kernels.

Considering both linear partitioning of droplet number and logarithmic partitioning of droplet mass, the above kernel was run for the initial droplet number spectrum (normalized to  $1 \text{ gm m}^{-3}$ ) used by Golovin (here on a logarithmic scale):

$$f(\ln r) = \frac{3v N_0}{v_0} \exp(-v/v_0) \quad (17)$$

where  $v$  is the volume of a drop of radius  $r$ ,  $v_0$  is the mean volume over the spectrum at  $t = 0$ , and  $N_0$  is the total number of drops per unit volume (also at  $t = 0$ ).

In Figure 1, the model mass spectrum after 1800 sec is compared to the exact analytic solution of Golovin for both cases of redistribution. It is clear that a linear partitioning of droplet number does result in an incorrect widening

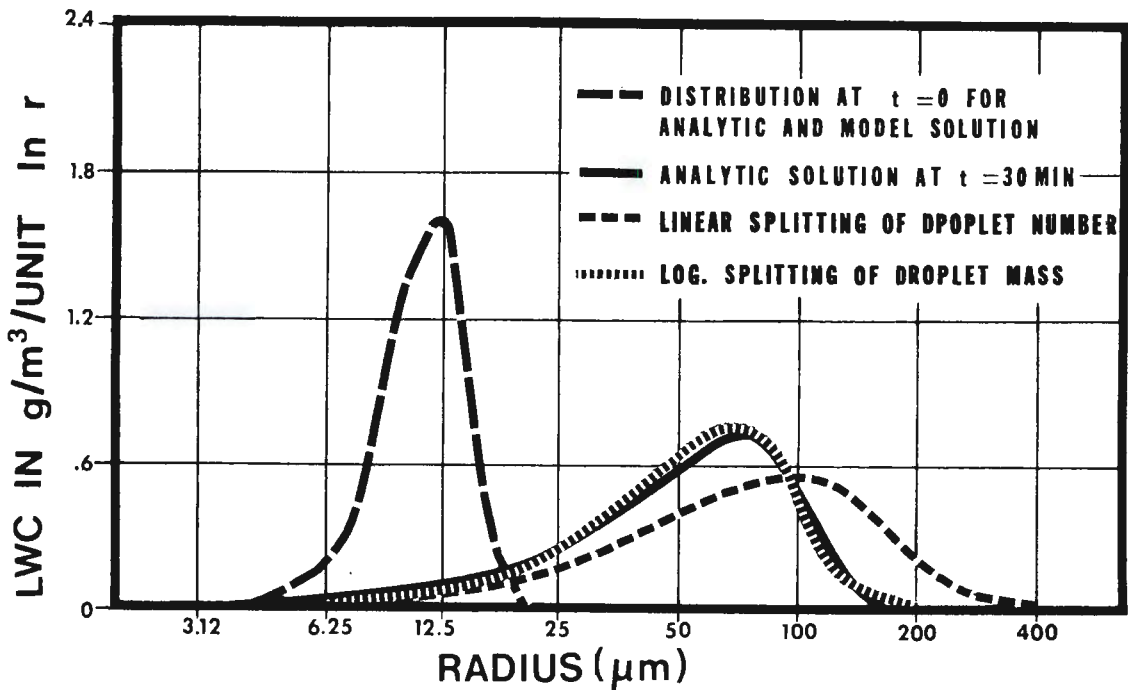


Figure 1. Analytic and model solutions to Golovin's sum of masses collection kernel.

of the distribution. Logarithmic partitioning of mass, however, results in a reasonably accurate final solution. As mentioned, partitioning of mass does not permit number conservation. However, a plot of the number spectra reveals that mass partitioning is still superior to linear splitting.

The constant kernel of Scott (1968) was also run for the initial spectrum given in Eq. (17). The relative comparisons (for the two cases) are very similar to the results generated by the Golovin kernel, with logarithmic partitioning of mass giving a better solution. On the basis of these results, logarithmic partitioning of mass was chosen for the "splitting" procedure.

## 8. COLLISION AND COALESCENCE EFFICIENCIES

Collision efficiencies for radii greater than 28  $\mu\text{m}$  are taken from Berry's (Berry, 1967) numerical fit of the Shafirir-Neiburger data (Shafirir and Neiburger, 1963). Efficiencies for radii smaller than 28  $\mu\text{m}$  are based on the calculations of Davis and Sartor (1967).

The coalescence efficiencies used for this study are based on the empirical work of Whelpdale and List (1971), and Levin et al. (1973). Whelpdale and List observed collisions between two drops, one of approximately 35  $\mu\text{m}$  radius and the other ranging from 500 to 1750  $\mu\text{m}$  in radius. This combination essentially describes hydrometeors collecting cloud droplets. They determined that, at least for collector drop radii  $400 < r_i < 2000 \mu\text{m}$  and collected droplet radii  $20 < r_n < 100 \mu\text{m}$ ,

$$E(i,n) = \frac{r_i^2}{(r_i + r_n)^2} = \frac{1.0}{(1 + r_n/r_i)^2} . \quad (18)$$

Levin et al. concentrated on collector droplets from 50 to 100  $\mu\text{m}$  in radius, with larger size ratios. Their data, together with that of Whelpdale and List, is shown in Figure 2. Their experimental points fall below the Whelpdale-List curve, but substantiate the downward trend with increasing droplet/drop ratio.

Two sets of coalescence efficiencies were taken from Figure 2 for the model experiments. The first (Case II) is the Whelpdale-List formulation, assuming that it applies over the entire range of cloud drop sizes. The second (Case III) is a formulation based on the combined data of Whelpdale and List, and Levin et al. (the dashed line extension in Figure 2). A third order least squares fit produced maximum errors of less than 2%:

$$E(i,n) = A(0) + A(1)P + A(2)P^2 + A(3)P^3,$$

where  $P = r_n/r_i$ ,

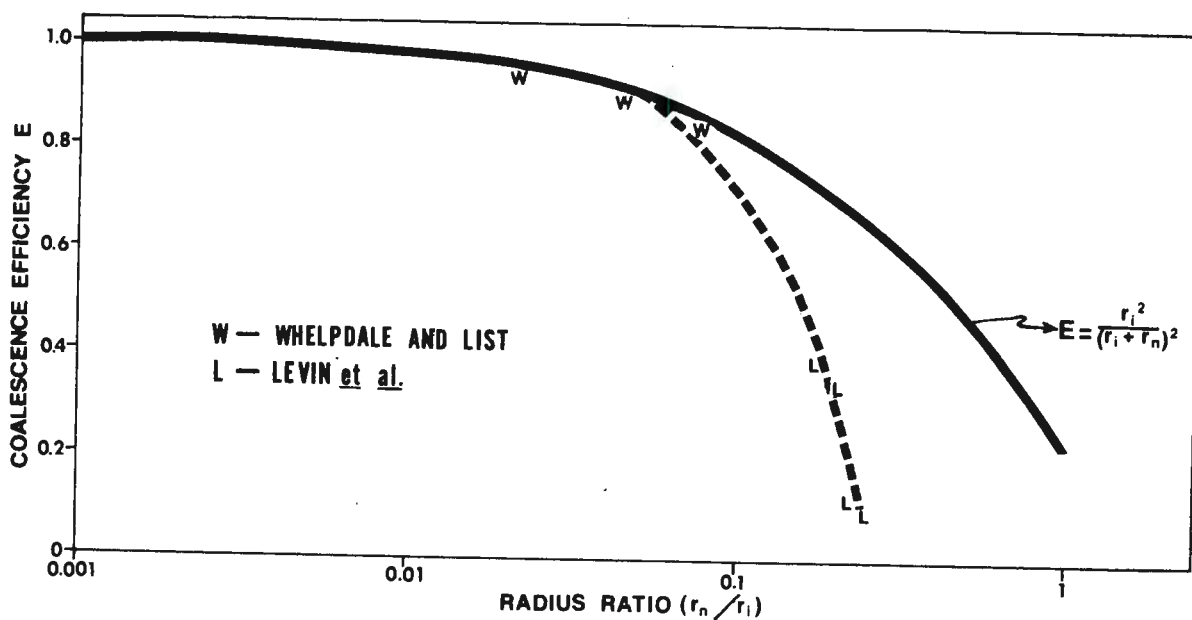


Figure 2. Experimentally derived values of coalescence efficiency as determined by Whelpdale and List (1971), and Levin et al. (1973). Solid line is the relation suggested by Whelpdale and List; dashed extension is that suggested by Levin et al.

$$A(0) = 0.9986810817,$$

$$A(1) = -1.786534384,$$

$$A(2) = -7.746074296,$$

and  $A(3) = -1.149299369.$

It is recognized that these data are incomplete and in need of further verification. The qualitative substantiation of Whelpdale and List's work by Levin et al., however, is significant for the following reason. It indicates that utilization of a coalescence efficiency affects, primarily, droplets of similar size.

Berry and Reinhardt (1973), in their continued development of improved parameterization schemes, recognized that the

growth of the hydrometeor phase is the result of two processes: accretion (hydrometeors collecting cloud droplets) and self-collection (hydrometeors collecting hydrometeors). While accretion can be approximated by continuous collection (average growth), Berry and Reinhardt point out that self-collection must be described by stochastic collection and can be quite important. Consequently, a reduction in collection growth as the result of incomplete coalescences primarily affects self-collection. It was the specific purpose of the study reported here to determine how the reduction of that component affects the initiation of precipitation from a warm cumulus. It can be demonstrated by existing theory that initiation can occur within the necessary time frame. The theory, however, assumes that all collisions result in coalescences.

## 9. DROP BREAKUP

The term  $\beta$  in Eq. (1) accounts for drop breakup. As used by Nelson (1971), the empirical work of D'Albe and Hicayetulla (1955) provide the data on which drop breakup is computed. They conducted experiments with large (4.5-6.0 mm radius) drops in order to determine the number and size of the breakup fragments. Fragment number and size are interpolated for their data in order to obtain a redistribution of liquid water for category 49 of the discrete sequence.

In wind tunnel tests Blanchard (1950) found that the size at which drops become unstable is a function of the degree of turbulence, but that extreme deformation occurs for drops larger than 2.5 mm radius. For this reason, 2820  $\mu\text{m}$  (category 49) was chosen as the largest radius in the discrete sequence. A drop entering this category is broken up into approximately 16 fragments and redistributed as shown by the histogram in Figure 3.

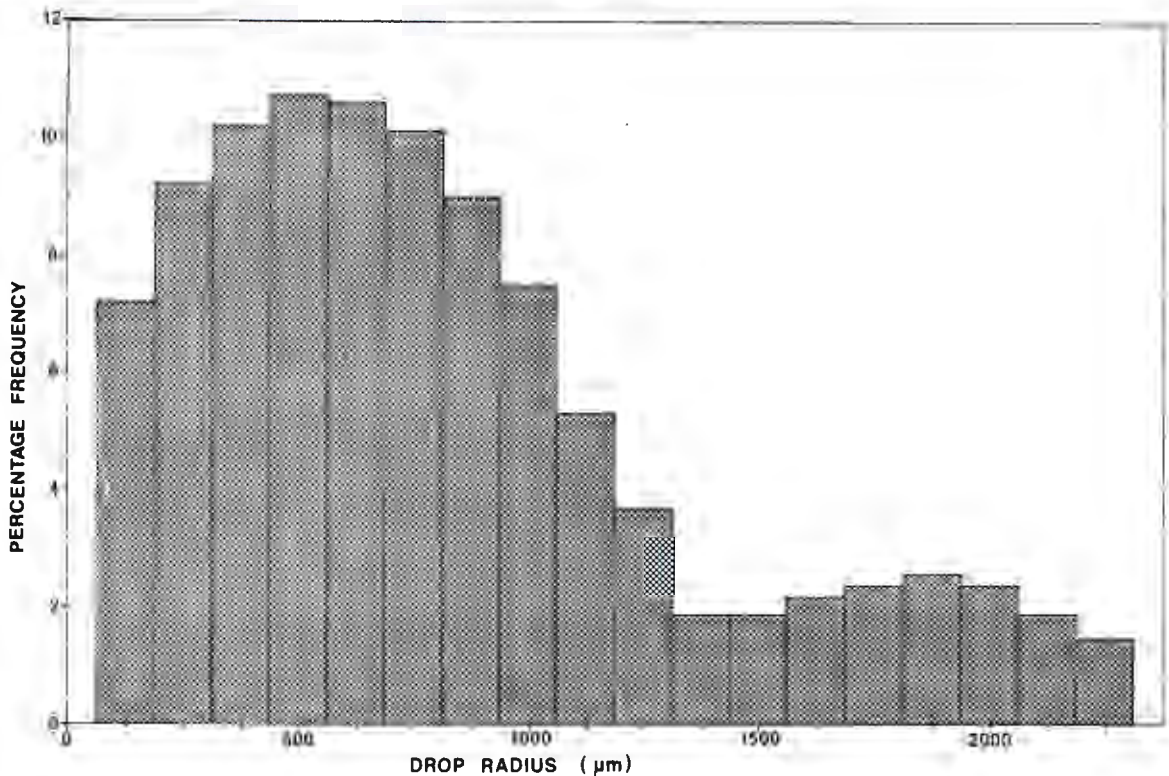


Figure 3. Redistribution pattern for drop breakup.

## 10. COMPUTATIONAL PROCEDURE

For a particular experiment, the following sequence of major events is followed by the model:

a) Data is read in for model initiation: cloud droplet spectra, Davis-Sartor collision efficiencies, updraft profile, as well as other bookkeeping information.

b) Shafir-Neiburger collision efficiencies, droplet terminal velocities, and coalescence efficiencies are calculated and stored for model use. Droplet size categories are set up; the input cloud droplet spectra are fit into these categories.

c) Collision-coalescence operates on droplet spectra.

d) Drops entering category 49 are broken into fragments and redistributed.

e) Droplets are advected between model levels.

f) Output of droplet spectra, liquid water contents, rain fallout at cloud base, etc. is given at specified time intervals for all ten levels of the model.

g) Steps (c) through (f) are repeated, at 5 second time steps, until the final time limit is reached. Experiments to be described were run for a minimum of 30 minutes cloud time.

### 3. INITIAL CLOUD CONDITIONS

For comparison and consistency purposes the same initial droplet spectrum and updraft profile as used by Nelson (1971) are utilized. The data of Braham et al. (1957) for tropical cumuli with no echoes are used for the initial spectra for all levels in the cloud. A liquid water content of  $0.8 \text{ gm m}^{-3}$ , an average value as measured by Braham et al., results in the water mass spectrum given in Figure 4. Initial number concentration is  $64 \text{ cm}^{-3}$ . Measured average droplet concentrations were  $48 \text{ cm}^{-3}$  for the non-echo cumuli.

As in Nelson, a  $\Delta z$  of 400 m is chosen. In this model 400 m results in a cloud depth of 3600 m. As mentioned previously, an additional level exists below cloud base into which rainfall is accumulated.

The time-independent updraft profile has a maximum speed of  $4 \text{ m sec}^{-1}$  at level 7 of the model, decreasing to zero at cloud base and top. The profile serves two purposes. It leads to a convergent zone above the profile maximum and thus an accumulation of water. Although the mechanism of accumulation is unrealistic from a continuity standpoint, liquid water increase with cloud height is consistent with increases produced as the result of the condensation process (assuming that the adiabatic value is not exceeded) and with observations (e.g., Warner, 1955). Secondly, the updraft profile provides a realistic restraint for hydrometeor fallout.

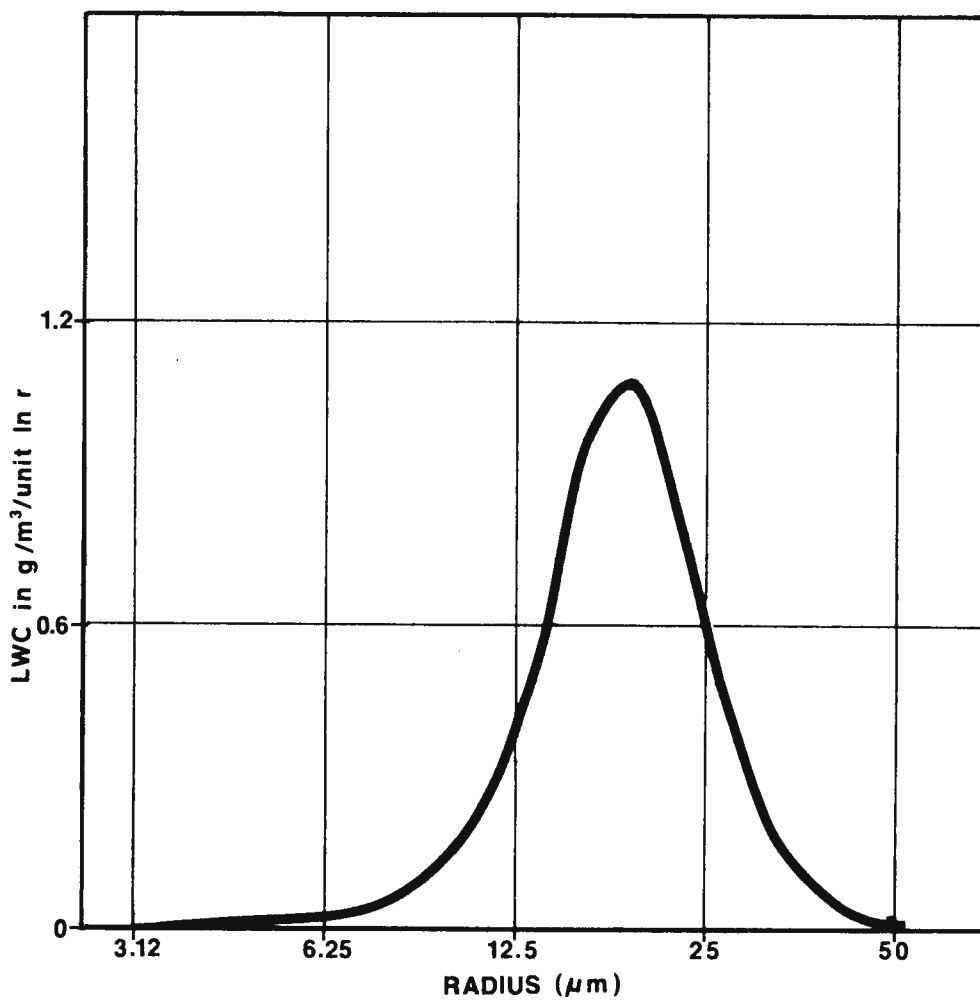


Figure 4. Initial cloud droplet mass distribution used in model experiments (LWC =  $0.8 \text{ gm m}^{-3}$ ).

#### 4. MODEL RESULTS

Three experiments were conducted to determine the relative effect of using the coalescence efficiencies. Case I is a control case, assuming a coalescence efficiency of one. Case II assumes coalescence efficiencies as calculated by the Whelpdale-List formula, Eq. (18), and Case III utilizes coalescence efficiencies taken from the combined data of Whelpdale and List, and Levin et al.

A set of three-dimensional diagrams of droplet mass spectral change offers a convenient method of observing changes in the droplet distribution with time and cloud height. Figure 5 shows spectral change for Case I, the control case. The slant axis (at each of the levels) is a logarithmic scale of droplet radius while each of the intersections of a droplet spectrum with the horizontal axis represents one minute of time. The vertical axis is a measure of liquid water content (LWC) under the curve. Consequently, at each of the model's ten levels a pictorial description of the droplet spectral evolution is presented. This evolution proceeds as the result of droplet movement between model levels (updraft plus droplet fall velocity) and movement along a spectral curve (collision-coalescence plus breakup).

As Nelson (1971) found, temporary accumulation of water at the top of the cloud leads to a generation zone for drops large enough to fall through the updraft profile. A maximum LWC of  $2.8 \text{ gm m}^{-3}$  exists at level 10 at about 7 minutes. The significance demonstrated by this control case lies in the fact that local temporary accumulations of only moderate size are enough to sufficiently initiate the collision-coalescence mechanism, leading to rain exiting cloud base in about 15 minutes (see Figure 5). Such moderately large LWC's are consistent with observations. Ackerman (1959), for example, found maximum water contents of over  $3 \text{ gm m}^{-3}$  in tropical cumuli of the depth simulated here. He also found that LWC's were

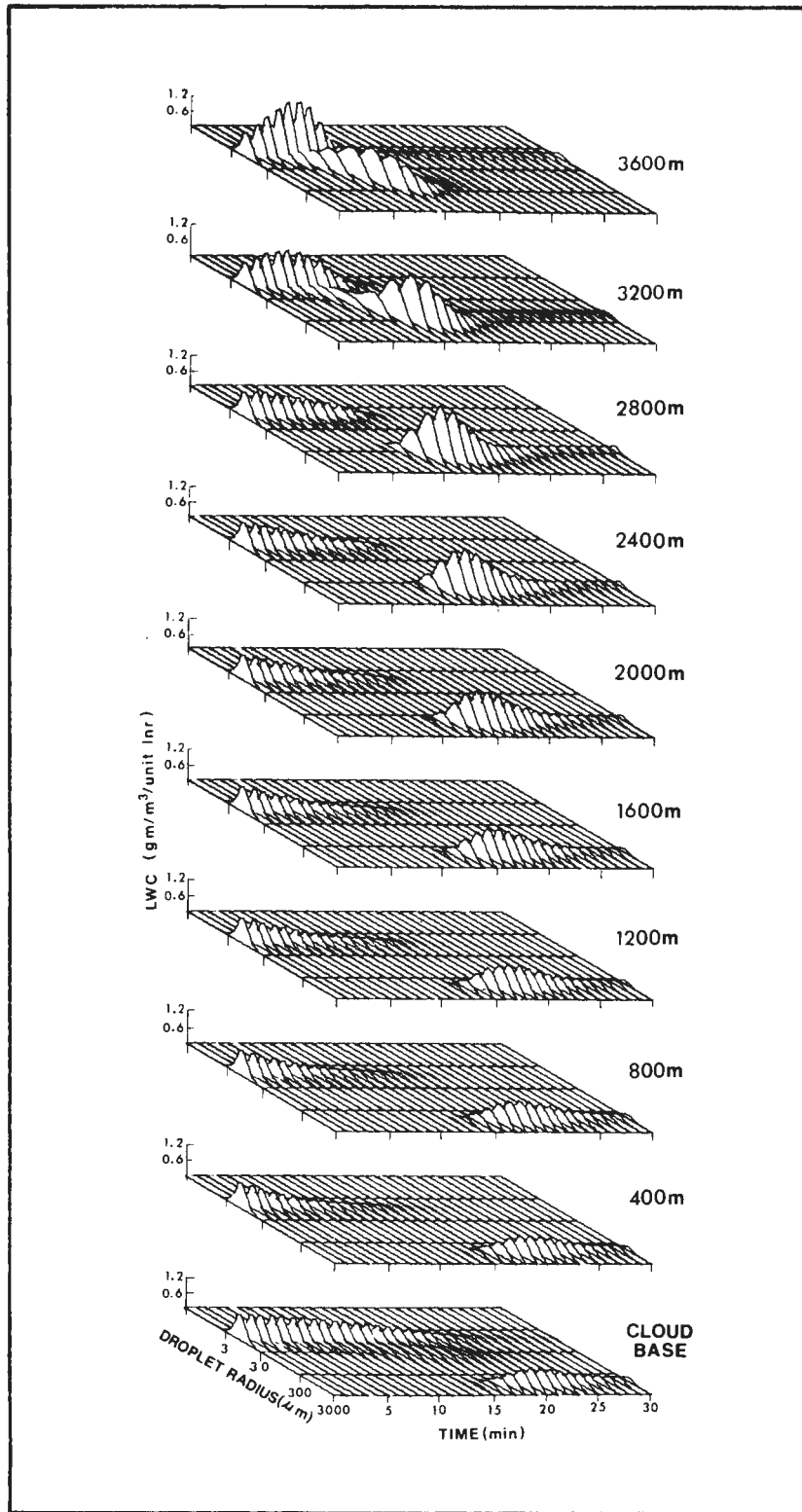


Figure 5. Droplet mass spectra as a function of time and height for Case I -- coalescence efficiencies equal to one.

successively larger with increased height.

The corresponding spectral diagrams for Cases II and III, shown in Figures 6 and 7, represent increasing limitations on droplet growth because of incomplete coalescences. The obvious change to be noted is the increasing accumulation of water at level 10, especially for Case III. The sharp decrease of coalescence efficiency (with increasing ratio), as shown in Figure 2, is responsible for this delayed growth in Case III.

Figure 8 is a time plot of LWC for level 10 for Cases II and III, together with the control, Case I. In all three cases, LWC rises until that point where collision-coalescence growth produces drop sizes with terminal velocities sufficient to penetrate the updraft. Simultaneously, the large LWC, which exists primarily in relatively small droplets, is quickly depleted by growth of these large particles (coalescence efficiencies remain close to one for small size ratios). Case II differs only slightly from the control; whereas the LWC rises to  $2.8 \text{ gm m}^{-3}$  for Case I, a maximum of  $3.6 \text{ gm m}^{-3}$  is reached for Case II. Spectral evolution at cloud top (for Cases I and II) is a continuous process, the second water maximum forming as an evolution from the primary maximum. This evolution is delayed two to three minutes as the result of the use of the Whelpdale-List formula.

Case III, however, because of its severe limitation on growth between drops of similar size, presents a very different situation. The LWC at level 10 rises to more than double that of the control. Development of large hydrometeors, when it does happen, does not progress as a continuous evolution from the bulk of liquid water. At about 20 minutes, large hydrometeors appear discontinuously when viewed on an LWC plot (as given in Figure 7).

Rainfall rate and cumulative rainfall are plotted in Figures 9 and 10. One might initially suspect that, although precipitation is delayed for Cases II and III, rainfall rate and total rainfall would be as large. Such is not the case.

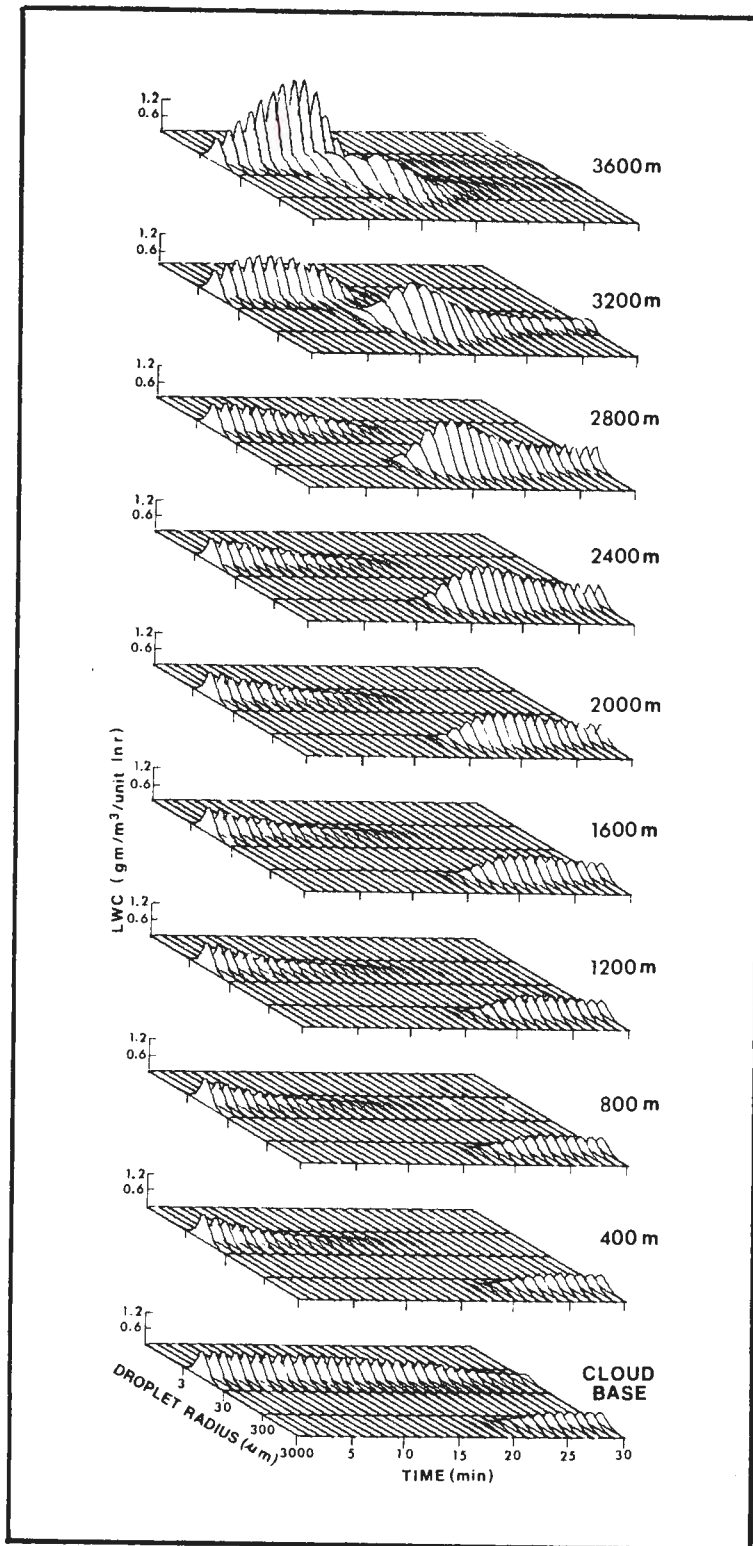


Figure 6. Droplet mass spectra as a function of time and height for Case II -- coalescence efficiencies as defined by the Whelpdale-List formula.

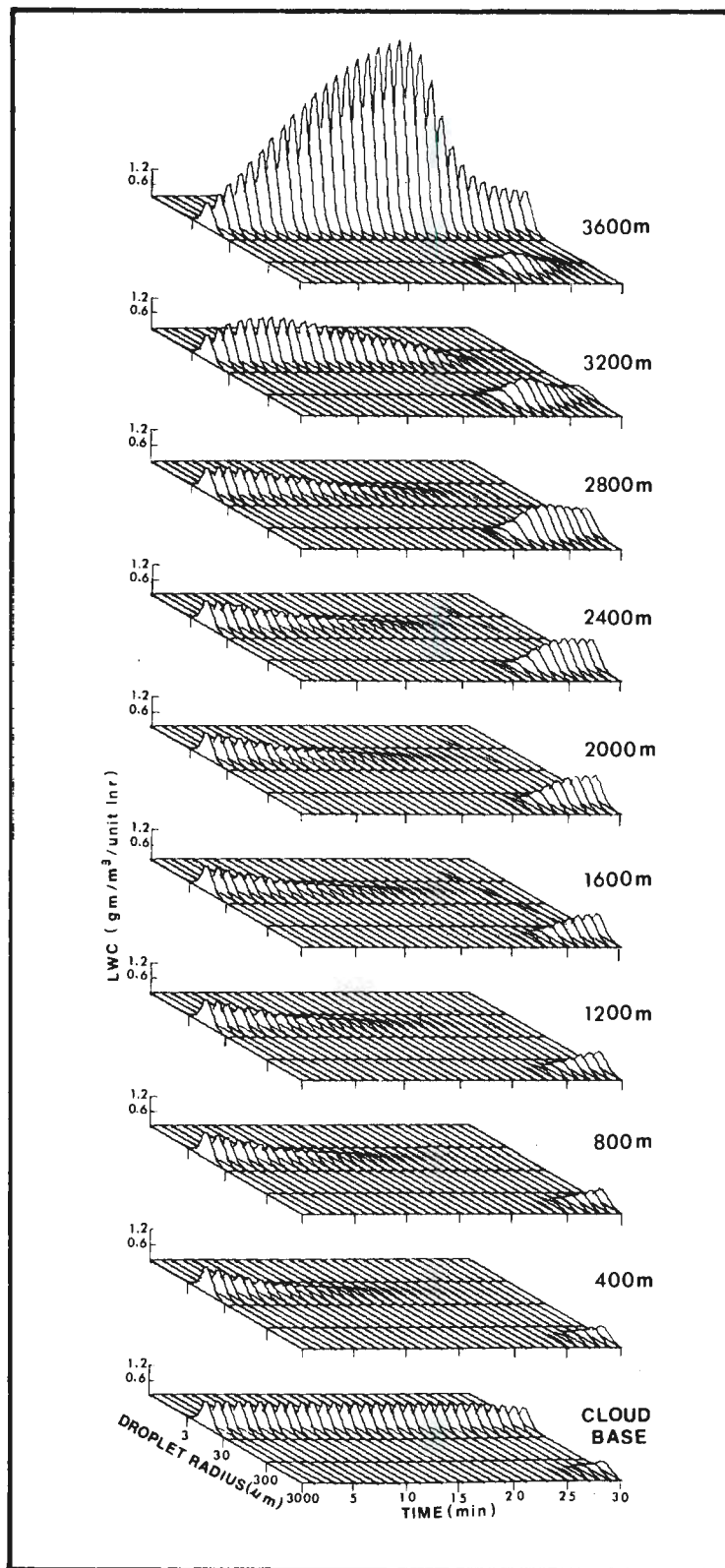


Figure 7. Droplet mass spectra as a function of time and height for Case III -- coalescence efficiencies as defined by the Whelpdale-List, Levin et al. combined data.

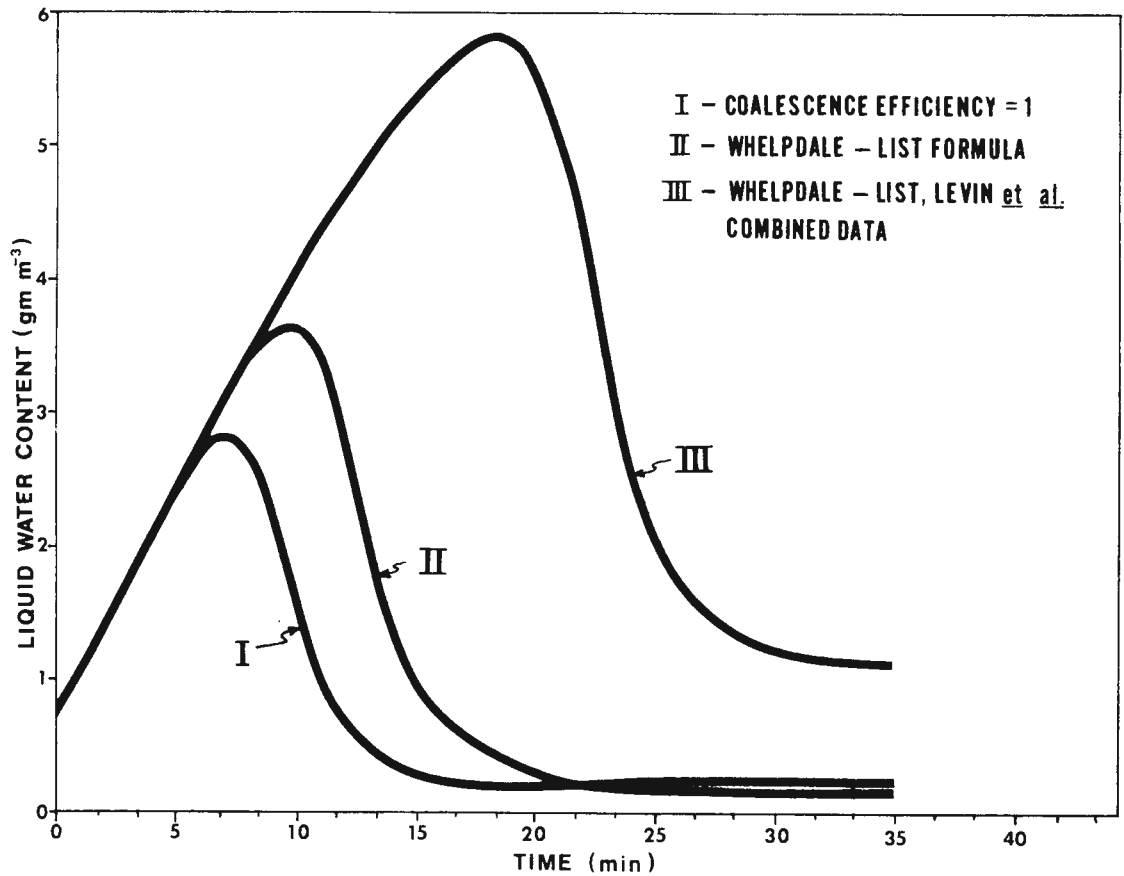


Figure 8. Liquid water content change at cloud top for Cases I, II, and III.

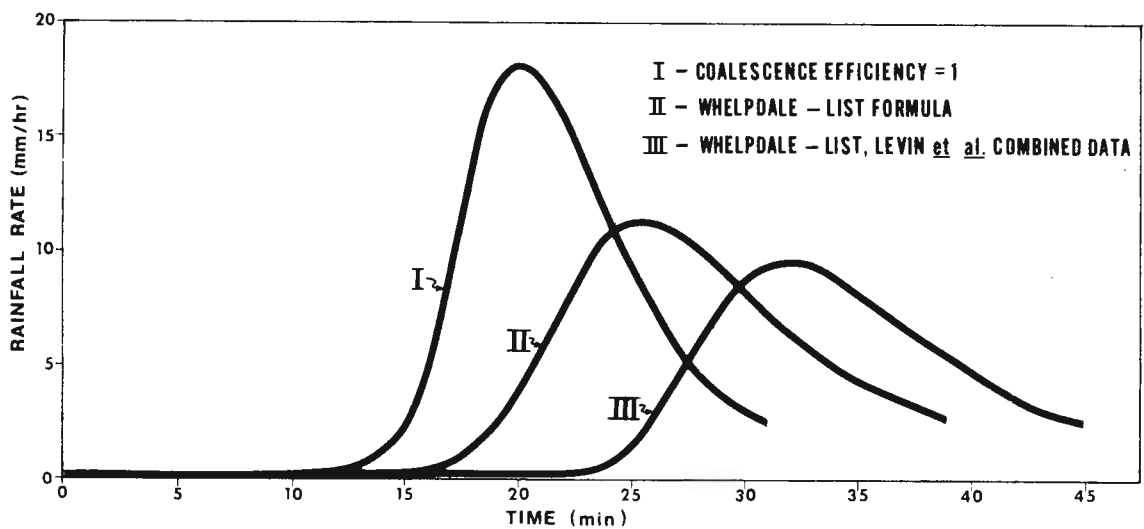


Figure 9. Rainfall rates for Cases I, II, and III.

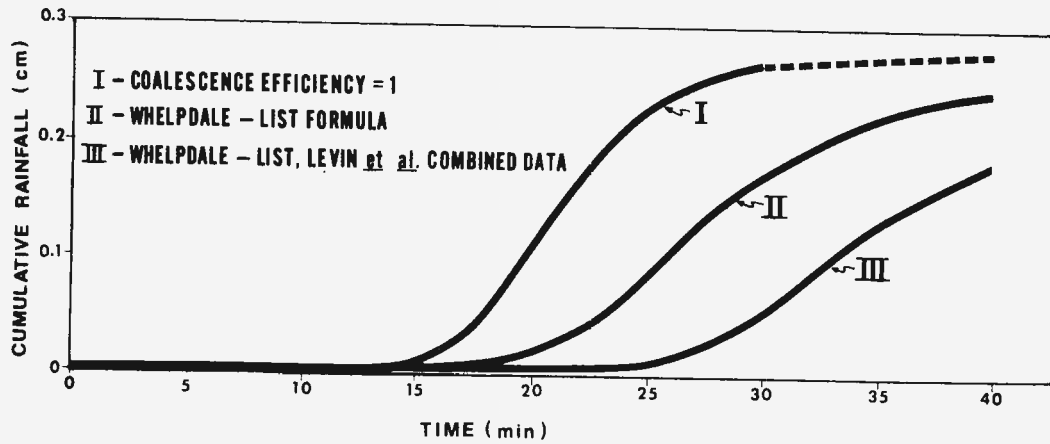


Figure 10. Cumulative rainfall for Cases I, II, and III.

Maximal rates of approximately 18, 11, and 9 mm hr<sup>-1</sup> occur at 20, 25, and 32 minutes for Cases I, II, and III, respectively. Similarly, cumulative rainfall is less for periods up to 40 minutes.

Raindrop size spectra for the three cases were compared to each other and against the Marshall-Palmer spectra (Marshall and Palmer, 1948). For rainfall rates common to the three cases it was found that the spectra differed only slightly from each other. In general, however, the spectra for Cases II and III were shifted toward smaller sizes. For example, Figure 11 shows comparative spectra at the rainfall rate which was maximum for Case III, 9.5 mm hr<sup>-1</sup>. The diagonal line is the Marshall-Palmer spectrum.

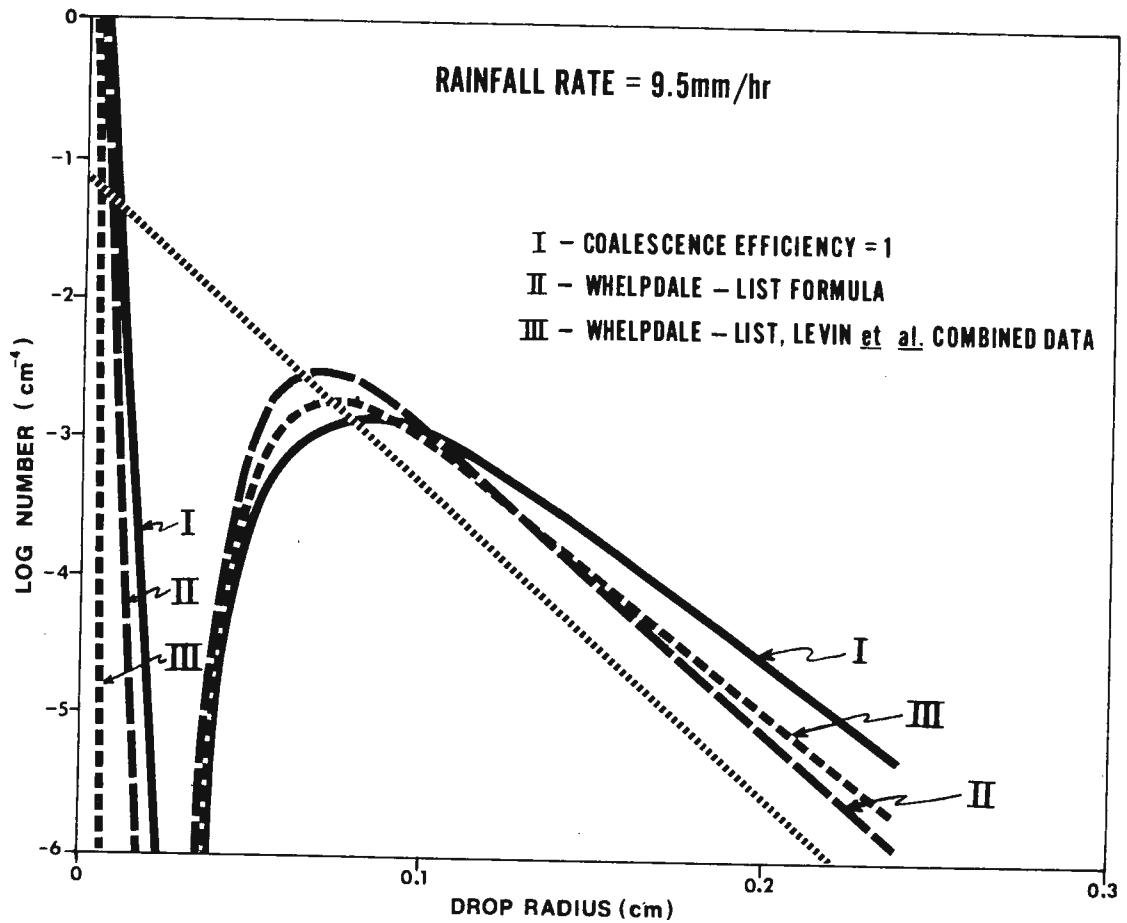


Figure 11. Raindrop spectra just above cloud base for a rainfall rate of 9.5 mm hr<sup>-1</sup> for Cases I, II, and III. Diagonal line is the Marshall-Palmer spectrum for that rate.

## 5. SUMMARY AND CONCLUSIONS

The stochastic theory of collision-coalescence has enabled cloud physics to explain production of rain from a warmer than freezing cloud within 20 minutes. Calculations which can demonstrate this occurrence, however, are based on the assumption that all collisions result in coalescences.

Recent empirical studies have determined that coalescence efficiency decreases with increasing size ratio of the two drops. A time-dependent one-dimensional model which incorporates the effects of stochastic coalescence, drop breakup, and vertical transfer by means of a constant updraft profile was used here to study the effect of using these efficiencies. Utilizing two separate sets of data which outline the suggested limits of empirical findings, comparisons were made to a control case in which rain could be generated from a tropical cumulus in about 15 minutes.

The results were found to be quite sensitive to coalescence efficiencies for collisions between droplets very close in size, the region in which the two sets of data differed. In general, however, utilization of these efficiencies leads to delay of precipitation and to decreases both in rainfall intensity and cumulative rainfall. For equivalent rates of rainfall, however, raindrop size spectra were found to differ only slightly. The most significant finding is the large LWC which is necessary to sufficiently stimulate the collision-coalescence mechanism for those cases where coalescences are restricted. Using the more restrictive set of coalescence efficiency data resulted in maximum LWC's which are unreasonably large and uncommon for typical tropical cumuli. If coalescence efficiencies are indeed as limited as this one set of empirical data indicate, then other compensating effects (e.g., electrical) must be found. It is suggested that more laboratory work be conducted to verify and extend the empirical results thus far determined.

## REFERENCES

- Ackerman, B., 1959: The Variability of the Water Contents of Tropical Cumuli. J. Meteor., 16, 191-198.
- Bartlett, J. T., 1966: The Growth of Cloud Droplets by Coalescence. Quart. J. R. Meteor. Soc., 92, 93-104.
- Bergeron, T., 1935: On the Physics of Cloud and Precipitation. Proc. 5th Assembly U.G.G.I. Lisbon, 2, p. 156.
- Berry, E. X., 1967: Cloud Droplet Growth by Collection. J. Atmos. Sci., 24, 688-701.
- \_\_\_\_\_, 1968: Modification of the Warm Rain Process. Preprints First Natl. Conf. Weather Modification, Albany, N. Y., Amer. Meteor. Soc., 81-88.
- \_\_\_\_\_, and R. L. Reinhardt, 1973: Modeling of Condensation and Collection Within Clouds. Final Report to the National Science Foundation on Grant GA-21350, 96 pp.
- Blanchard, D. G., 1950: The Behavior of Water Drops at Terminal Velocity in Air. Trans. Amer. Geophys. Un., 31, 836-842.
- Braham, R. R., L. J. Battan, and H. R. Byers, 1957: Artificial Nucleation of Cumulus Clouds. Meteor. Monogr., 2, No. 11, 47-85.
- Bowen, E. G., 1950: The Formation of Rain by Coalescence. Aust. J. Sci. Res., 3, 193-213.
- D'Albe, E. M., and M. S. Hidayetulla, 1955: The Breakup of Large Water Drops Falling at Terminal Velocity in Free Air. Quart. J. R. Meteor. Soc., 81, 610-613.
- Danielsen, E. F., R. Bleck, and D. A. Morris, 1972: Hail Growth by Stochastic Collection in a Cumulus Model. J. Atmos. Sci., 29, 135-155.
- Davis, M. H., and J. D. Sartor, 1967: Theoretical Collision Efficiencies for Small Cloud Droplets in Stokes Flow. Nature, 215, 1371-1372.
- Findeisen, W., 1939: Zur Frage der Regentropfenbildung in reinen Wasserwolken. Met. Z., 56, p. 365.

- Golovin, A. M., 1963: The Solution of the Coagulation Equation for Cloud Droplets in a Rising Air Current. Bull. Acad. Sci., USSR, Geophys. Ser., No. 5, 783-791.
- Gunn, R., and G. D. Kinzer, 1949: The Terminal Velocity of Fall for Water Droplets in Stagnant Air. J. Meteor., 6, 243-248.
- \_\_\_\_\_, and W. Hitschfeld, 1951: A Laboratory Investigation of the Coalescence Between Large and Small Water-Drops. J. Meteor., 8, 7-16.
- Hocking, L. M., 1959: The Collision Efficiency of Small Drops. Quart. J. R. Meteor. Soc., 85, 44-51.
- Jayarathne, O. W., and B. J. Mason, 1964: The Coalescence and Bouncing of Water Drops at an Air/Water Interface. Proc. Roy. Soc., London, A, 280, 545-565.
- Kessler, E., 1969: On the Distribution and Continuity of Water Substance in Atmospheric Circulation. Meteor. Monogr., 10, No. 32, 84 pp.
- Kovetz, A., and B. Olund, 1969: The Effect of Coalescence and Condensation on Rain Formation in a Cloud of Finite Vertical Extent. J. Atmos. Sci., 26, 1060-1065.
- Langmuir, I., 1948: The Production of Rain by a Chain Reaction in Cumulus Clouds at Temperatures above Freezing. J. Meteor., 5, 175-192.
- Levin, Z., M. Neiburger, and L. Rodriguez, 1973: Experimental Evaluation of Collection and Coalescence Efficiencies of Cloud Drops. J. Atmos. Sci., 30, 944-946.
- Ludlam, F. H., 1951: The Production of Showers by the Coalescence of Cloud Droplets. Quart. J. R. Meteor. Soc., 77, 402-417.
- Magono, C., and T. Nakamura, 1959: On the Behavior of Water Droplets during Collision with a Large Water Drop. J. Meteor. Soc. Japan, ser. 2, 37, 124-127.
- Marshall, J. S., and W. McK. Palmer, 1948: The Distribution of Raindrops with Size. J. Meteor., 5, 165-166.
- Nelson, L. D., 1971: A Numerical Study on the Initiation of Warm Rain. J. Atmos. Sci., 28, 752-762.

- Pearcey, T., and G. W. Hill, 1956: A Theoretical Estimate of the Collection Efficiencies of Small Droplets. Quart. J. R. Meteor. Soc., 83, 77-92.
- Sartor, D., 1954: A Laboratory Investigation of Collision Efficiencies, Coalescence and Electrical Charging of Simulated Cloud Droplets. J. Meteor., 11, 91-103.
- Schotland, R. M., and E. J. Kaplin, 1956: The Collision Efficiency of Cloud Droplets. New York Univ. Met. Dept. Rep. No. AFCRC-TH-55-867, 34 pp.
- Scott, W. T., 1968: Analytical Studies of Cloud Droplet Coalescence. J. Atmos. Sci., 25, 54-65.
- Shafir, U., and M. Neiburger, 1963: Collision Efficiencies of Two Spheres Falling in a Viscous Medium. J. Geophys. Res., 68, 4141-4148.
- Silverman, B. A., and M. Glass, 1973: A Numerical Simulation of Warm Cumulus Clouds: Part I. Parameterized vs Non-Parameterized Microphysics. J. Atmos. Sci., 30, 1620-1637.
- Simpson, J., and V. Wiggert, 1969: Models of Precipitating Cumulus Towers. Mon. Wea. Rev., 97, 471-489.
- Takeda, T., 1971: Numerical Simulation of a Precipitating Convective Cloud: The Formation of a "long-lasting" Cloud. J. Atmos. Sci., 28, 350-376.
- Telford, J. W., 1955: A New Aspect of Coalescence Theory. J. Meteor., 12, 436-444.
- \_\_\_\_\_, N. S. Thorndike, and E. G. Bowen, 1955: The Coalescence between Small Water Drops. Quart. J. R. Meteor. Soc., 81, 241-250.
- \_\_\_\_\_, and N. S. Thorndike, 1961: Observations of Small Drop Collisions. J. Meteor., 18, 382-387.
- Thoman, D. C., and A. A. Szewczyk, 1966: Numerical Solutions of Time Dependent Two-Dimensional Flow of a Viscous Incompressible Fluid Over Stationary and Rotating Cylinders. TR 66-14, Univ. of Notre Dame, Notre Dame, Indiana.
- Twomey, S. 1964: Statistical Effects in the Evolution of a Distribution of Cloud Droplets by Coalescence. J. Atmos. Sci., 21, 553-557.

BEST  
AVAILABLE COPY

Warner, J., 1955: The Water Content of Cumuliform Cloud. Tellus, 7, 449-457.

Weinstein, A. I., 1970: A Numerical Model of Cumulus Dynamics and Microphysics. J. Atmos. Sci., 27, 246-255.

Whelpdale, D. M., and R. List, 1971: The Coalescence Process in Raindrop Growth. J. Geophys. Res., 76, 2836-2856.

Wobus, H. B., F. W. Murray, and L. R. Koenig, 1971: Calculation of the Terminal Velocity of Water Drops. J. Appl. Meteor., 10, 751-754.

BEST  
AVAILABLE COPY